

Conductance and selectivity fluctuations in D127 mutants of the bacterial porin OmpF

Henk Miedema · Maarten Vrouenraets ·
Jenny Wierenga · Bob Eisenberg · Tilman Schirmer ·
Arnaud Baslé · Wim Meijberg

Received: 20 April 2006 / Revised: 30 May 2006 / Accepted: 26 June 2006
© EBSA 2006

Abstract A recent molecular dynamics study questioned the protonation state and physiological role of aspartate 127 (D127) of *E. coli* porin OmpF. To address that question we isolated two OmpF mutants with D127 either neutralized (D127N) or replaced by a positively charged lysine (D127K). The charge state of the residue at position 127 has clear effects on both conductance and selectivity. The D127K but not the D127N mutant expresses resilient conductance and selectivity fluctuations. These fluctuations reflect, we think, either changes in the ionization state of K127 and/or transitions between unstable subconformations as induced by the electrostatic repulsion between two positively charged residues, K127 and the nearby R167. Our results slightly favor the view that in WT OmpF residue D127 is deprotonated. As for the role of D127 in OmpF functionality, the gating of both mutants shows very similar sensitivity toward voltage as WT OmpF. Moreover, the current fluctuations of the D127K mutant were observed also in the absence of an

applied electric field. We therefore dismiss D127 as a key residue in the control mechanism of the voltage-dependent gating of OmpF.

Keywords Current fluctuations · OmpF D127 mutant · Ion selectivity · OmpF Loop L3

Introduction

The outer membrane porin OmpF from *E. coli* was one of the first membrane proteins of which the X-ray crystal structure was resolved at high resolution (Cowan et al. 1992). OmpF forms a β -barrel-based structure with the 16 anti-parallel strands connected by turns at the periplasmic side and loops at the extracellular side (Delcour 2003; Klebba and Newton 1998; Schirmer 1998; Schulz 2002). One of the eight extracellular loops (L3) folds into the pore lumen. In the constriction zone, approximately half way down the channel, an aspartate (D113) and glutamate (E117) at the tip of L3 face an arginine cluster located at the channel wall (R42, R82 and R132) (Fig. 1). These five charged amino acid residues determine to a large extent the ion selectivity of the channel (Bredin et al. 2002; Danelon et al. 2003; Phale et al. 2001; Saint et al. 1996; Saxena et al. 1999), though residues located outside the eyelet contribute as well (Philippsen et al. 2002). OmpF also gates and the opening and closing is sensitive to the membrane potential (Bainbridge et al. 1998; Van Gelder et al. 1997; Phale et al. 1997; Robertson and Tielman 2002; Schindler and Rosenbusch 1978).

Electrostatic interactions play a key role in ion channel functionality (Eisenberg 1996a, b). The role of electrostatics in OmpF is evident from the sensitivity of

H. Miedema (✉) · M. Vrouenraets · J. Wierenga · W. Meijberg
Biomade Technology Foundation, Nijenborgh 4,
9747 AG Groningen, The Netherlands
e-mail: miedema@biomade.nl

B. Eisenberg
Department of Molecular Biophysics and Physiology,
Rush University Medical Center, 1750 W. Harrison Street,
Suite 1291, Chicago, IL 60612, USA

T. Schirmer · A. Baslé
Division of Structural Biology, Biozentrum,
University of Basel, Klingelbergstrasse 70,
4056 CH Basel, Switzerland

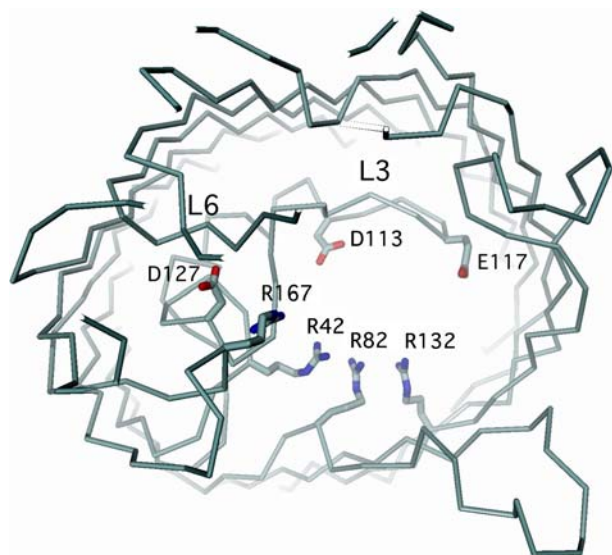


Fig. 1 Cross-section of a single WT OmpF porin at the height of the constriction zone and with the positions of *D127*, at the root of loop *L3*, and *R167*, at the root of loop *L4*, indicated

selectivity and gating to pH and ionic strength as both parameters affect the electrostatic profile of the pore lumen (Alcaraz et al. 2004; Baslé et al. 2004; Nestorovich et al. 2003; Saint et al. 1996; Todt and McGroarty 1992; Todt et al. 1992). As for selectivity, in general, the more negative the net charge of, especially, the constriction zone, the more cation selective the channel and vice versa (Vrouenraets et al. 2006). The picture that arises from gating studies is less clear. So far, all efforts to correlate the net charge of the eyelet to the gating properties of OmpF failed (Phale et al. 2001).

Brownian dynamics (Phale et al. 2001; Schirmer and Phale 1999) and molecular dynamic studies (Danelon et al. 2003; Im and Roux 2002a, b; Tieleman and Berendsen 1998) have contributed considerably to a better understanding of the role of electrostatics in OmpF functionality. BD and MD simulations require knowledge of the protonation state of all the basic and acidic residues. Incorrect charge states of particular residues may lead to inconsistencies of structure derived from the crystallization (at 77 K) and BD/MD simulations (at 310 K). For instance, the assignment of incorrect protonation states to residues D312 and E296 of OmpF during MD simulations resulted in a significantly smaller cross-sectional area at the constriction zone than that implicated by its crystal structure (Varma et al. 2006).

The actual pK value of an amino acid residue depends not only on pH and its intrinsic pK (as in free solution) but in addition also on charged residues in close proximity (Alcaraz et al. 2004; Cymes et al. 2005; Karshikoff et al. 1994; Varma and Jakobsson 2004).

The calculation of the contribution of the dielectric environment to the pK requires a value for the dielectric constant (ϵ) (Alcaraz et al. 2004; Karshikoff et al. 1994; Nestorovich et al. 2003; Varma and Jakobsson 2004). Of all the titratable residues considered, the calculation of the pK of D127 appears to be extremely sensitive to the value of ϵ and ranges from 4.9 (with $\epsilon = 20$) to > 14 (with $\epsilon = 4$) (Varma and Jakobsson 2004). Residue D127 is located at the root of loop L3 (Fig. 1). Its position and the uncertainty regarding its charge state make D127 an interesting candidate to be involved (somehow) in the gating and/or selectivity of OmpF. The present study aims to shed some more light on the role of D127 in OmpF functioning, and by doing so to identify its ionization state under physiological conditions. We isolated two D127 mutants, D127N and D127K, and explored their permeation and gating properties in solutions of different pH and ionic strength. In addition, we addressed the accessibility of residue D127 by trying to chemically modifying a D127C mutant with the cysteine-dependent MTSEA and MTSET reagents.

Materials and methods

The procedures for site-directed mutagenesis, isolation and purification of OmpF have been described in detail previously (Miedema et al. 2004). In short (mutated) OmpF monomer was purified from inclusion bodies in large amounts. Subsequent *in vitro* refolding led to a mixture of mono-, di- and trimeric protein, from which the latter was isolated with a yield of 5–10 mg per liter cell culture.

Chemical modification

The chemical modification was performed as in Vrouenraets et al. (2006). In short, the methanethio-sulfonate-based labels [2-(trimethylammonium)ethyl]-methanethiosulfonate (MTSET) and 2-aminoethylmethanethiosulfonate (MTSEA) were purchased from Anatrace (Maumee, OH, USA). Chemical modification was achieved after overnight incubation of 5–10 $\mu\text{g/ml}$ mutant OmpF with 50 mM MTS reagents in a 100 mM NaP_i buffer, pH 7.5, containing 0.3% *n*-octyl-polyoxyethylene (OPOE) detergent (Alexis Biochemicals, San Diego, CA, USA).

Electrophysiology

The detailed description of the entire procedure can be found in Miedema et al. (2004). Briefly, Planar Lipid

Bilayer (PLB) experiments were performed using a chamber and Delrin cuvette (Warner Inst., Hamden, CT, USA). By means of 3 M KCl/2% agar salt bridges, the *Cis* compartment was connected to the headstage of the Axopatch 200B amplifier (Axon Instruments, Foster City, CA, USA) and the *Trans* compartment was connected to ground. The PLB was painted across a 250 μm diameter aperture and was composed of phosphatidylethanolamine (PE) and phosphatidylcholine (PC), in an 8:2 ratio (v/v) and dissolved in *n*-decane. While stirring, $\sim 0.2 \mu\text{l}$ of a 1–10 $\mu\text{g/ml}$ OmpF stock solution (in 0.1 M KCl buffer supplemented with 1% OPOE) was added to the *Trans* side. Conductance (g) is defined as the trimeric slope conductance at 0 mV and calculated in between -10 and 10 mV, as recorded in symmetrical 0.1 M KCl solution. Data were low-pass filtered and digitized at 1 and 5 kHz, respectively.

Unless stated otherwise, chemicals, including PE and PC, were purchased from Sigma. All recording buffers contained, apart from NaCl, KCl or CaCl_2 , 20 mM HEPES ($\text{pK} = 7.4$) or 20 mM CAPS ($\text{pK} = 10.4$) and were adjusted with *n*-methyl-D-glucamine to pH 7.4 or 11, respectively. Gradients are represented *Cis//Trans*; for instance, a 0.1//1 M NaCl gradient indicates 0.1 M NaCl in the *Cis* compartment and 1 M NaCl in the *Trans* compartment. Reversal potentials measured in 0.01//0.1 or 1//0.1 M gradients NaCl have been corrected for liquid junction potentials of -11 and 11 mV, respectively. Selectivity was assessed in NaCl because OmpF expresses a higher selectivity in NaCl than in KCl (Vrouenraets et al. 2006). Conductance measurements, on the other hand, were performed in KCl because the conductance in KCl is significantly higher than in NaCl (Miedema et al. 2004).

Results

Differences between WT and mutant OmpF were most pronounced when recording at constant potential. Fig. 2 shows current traces at either -50 or 50 mV. The trimeric current level of WT OmpF (Fig. 2a) shows very little variation at these potentials. The calculated trimeric conductances in 0.1 M KCl of 661 pS at -50 mV and 721 pS at 50 mV are indicated in Fig. 2a. The difference between these two levels reflects the slight current rectification of WT OmpF (Nestorovich et al. 2003; Alcaraz et al. 2004).

Current traces of the D127N mutant are shown in Fig. 2b. On a rather rare occasion, we observed a conductance change as shown here at 50 mV, from 788 to

700 pS. Similar conductance changes but larger in magnitude and on a much more frequent basis were observed in the D127K mutant (Fig. 2c). This mutant switches resiliently between distinct current levels, both at negative and positive potentials. The all-points histograms in Fig. 2d, e, derived from D127K recordings at -50 and 50 mV, indicate two major conductance levels of 516 and 620 pS (at -50 mV) and 587 and 736 pS (at 50 mV).

Fig. 3a shows the effect of high ionic strength (1 M KCl, pH 7.4) on D127K behavior. This condition strongly inhibits the current to fluctuate, possibly due to strongly reduced electrostatic interactions. A similar result at low ionic strength can be achieved by raising the pH to 11 (Fig. 3b). We take this result as evidence that pH 11 promotes the deprotonation of K127 (the pK of a lysine in free solution is 10.4; but see Sect. 'Discussion'). As a result, this mutant starts to behave very much the same way as the D127N mutant. Note, for example, the small conductance step of D127K in Fig. 3b at 50 mV, very similar to the one observed in the D127N mutant at pH 7.4 (Fig. 2b). Compared to the conductance level in 0.1 M KCl, pH 7.4 (Fig. 2c), the conductance at pH 11 was increased by 25–33%. A similar pH-induced increase of conductance was observed in WT OmpF (data not shown) and has been reported previously (Todt and McGroarty 1992). Although divalent cations screen negative charges more effectively than monovalent cation species, 0.1 M CaCl_2 does not suffice to suppress D127K current transitions (Fig. 3c). Only in 1 M CaCl_2 (Fig. 3d) are the fluctuations reduced to the same level as in 1 M KCl (Fig. 3a). Figure 3c shows differences in frequency and dwell times of the fluctuations between the recordings at -50 and 50 mV. The trimeric nature of OmpF does not allow a quantitative dwell time analysis but what became clear is that these differences are not Ca^{2+} specific. Occasionally, similar behavior was observed in 0.1 M KCl (see, e.g., Fig. 7).

To test the voltage dependence of these current fluctuations, recordings were repeated at 0 mV and with an asymmetrical salt gradient of 1//0.1 M KCl as driving force (equivalent to ~ 52 mV). As the diffusion potential of a 1//0.1 M KCl gradient is just 1.1 mV, these recordings were thus performed in the virtual absence of an electric field. As shown in Fig. 4, under these conditions both mutants behave very much the same way as in symmetrical 0.1 M KCl solutions with an applied electrical potential of 50 mV (Fig. 2b, c). Apparently, these current fluctuations of D127K do not require per se the presence of an electric field across the membrane. In addition, both D127 mutants have retained their ability to respond to the membrane potential.

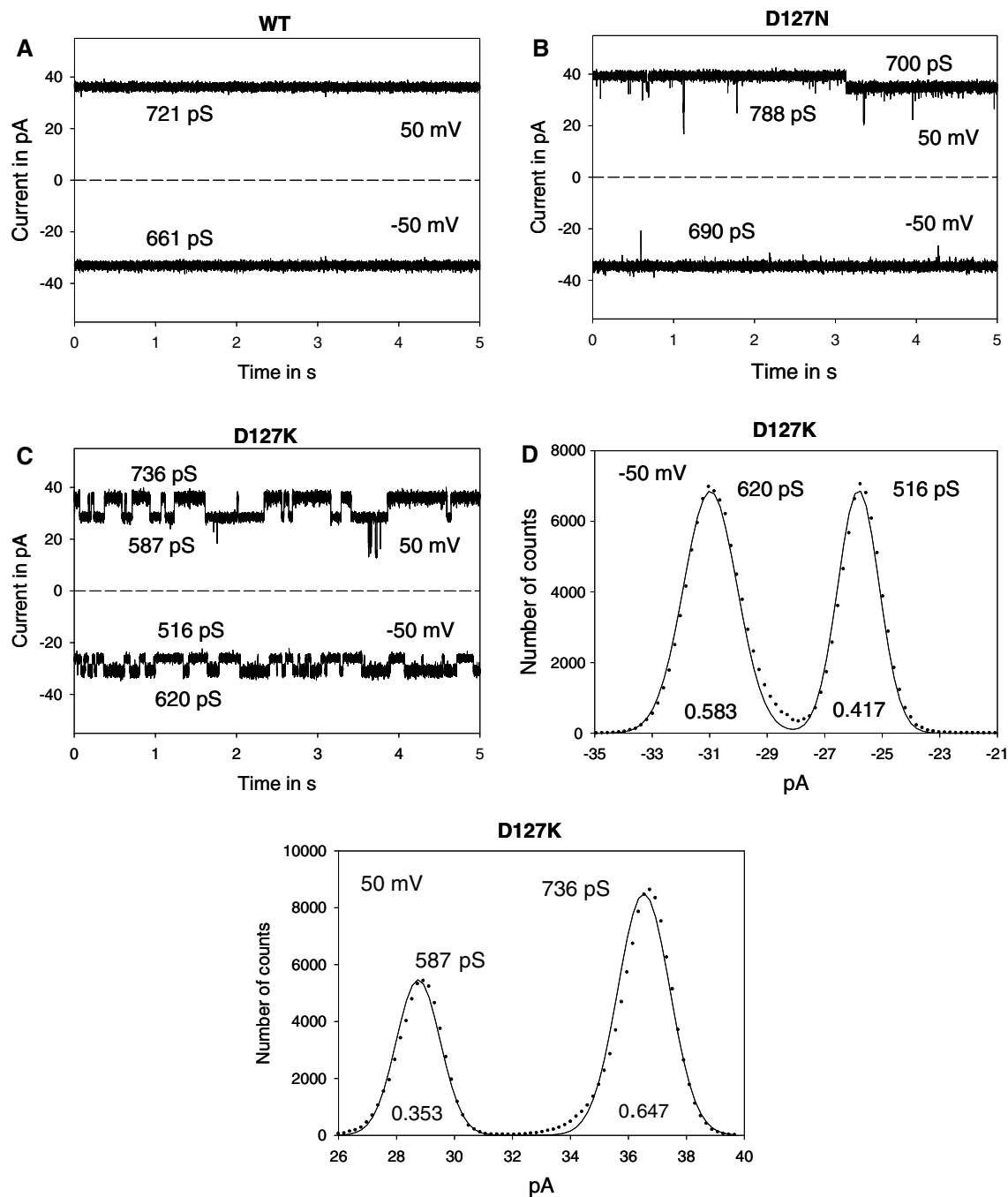


Fig. 2 Current traces of WT (**a**), D127N (**b**) and D127K (**c**) in 0.1 M KCl, pH 7.4, at a constant potential of either -50 or 50 mV. The indicated conductance levels of the D127K mutant were derived from Gaussian fits through the data of the all-points histograms in **d** (at -50 mV) and **e** (at 50 mV). Both *histograms* are

based on a total recording time of 30 s (150,000 counts in total) and plotted at a bin width of 0.195 pA. *Numbers* at the base line indicate relative probabilities as calculated from the surface areas under the two peaks

Fig. 5 shows current responses of D127N and D127K to a voltage ramp protocol in which the voltage was swept (10 mV/s) from 0 to ± 150 mV and then back to 0 mV. The bell-shaped voltage sensitivity of the two mutants and WT OmpF is very similar (at least at the qualitative level): they open at potentials in the range of

approximately -100 to 100 mV and close at more negative and more positive potentials. Note that the D127K trace of Fig. 5b shows the voltage-independent current fluctuations superimposed on the typical voltage gating of OmpF (this is most clearly seen in between -100 and -40 mV).

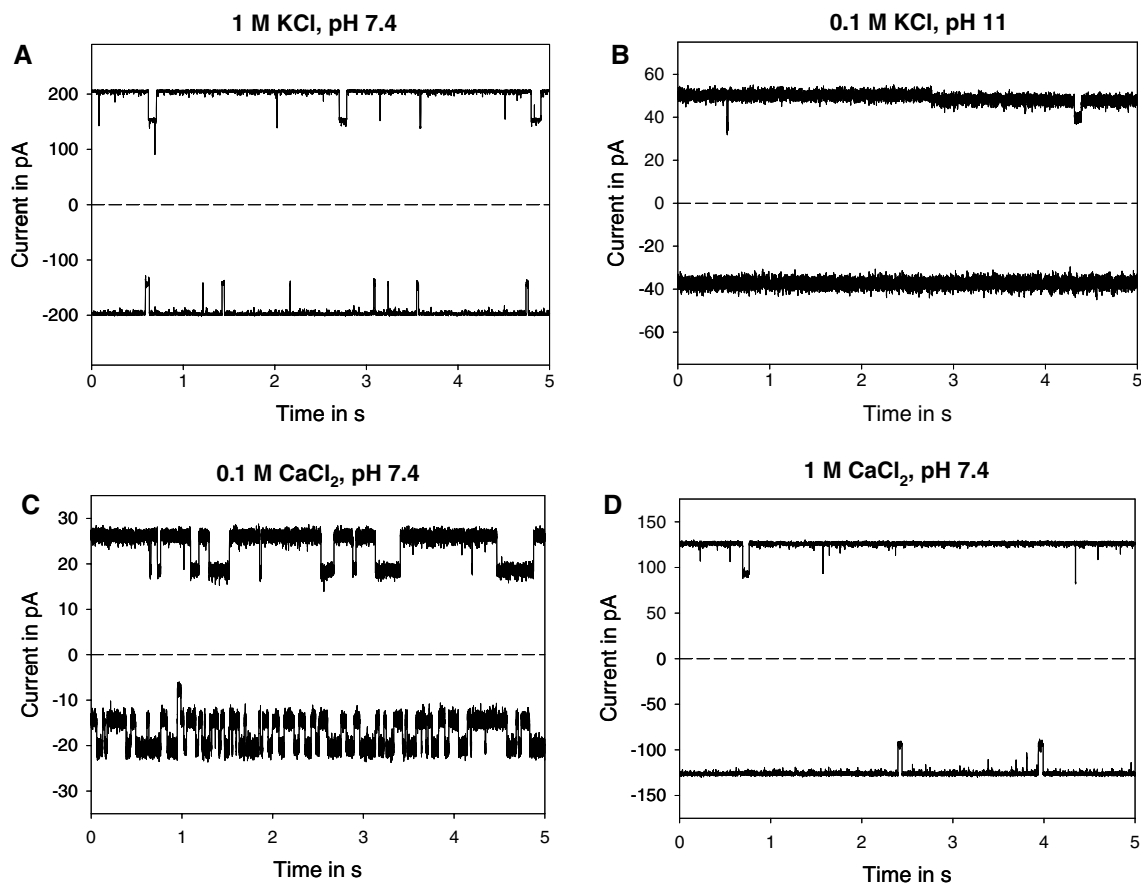


Fig. 3 Effect of 1 M KCl (a), pH 11 (b), 0.1 M CaCl₂ (c) and 1 M CaCl₂ (d) on D127K behavior (at ± 50 mV, as in Fig. 2)

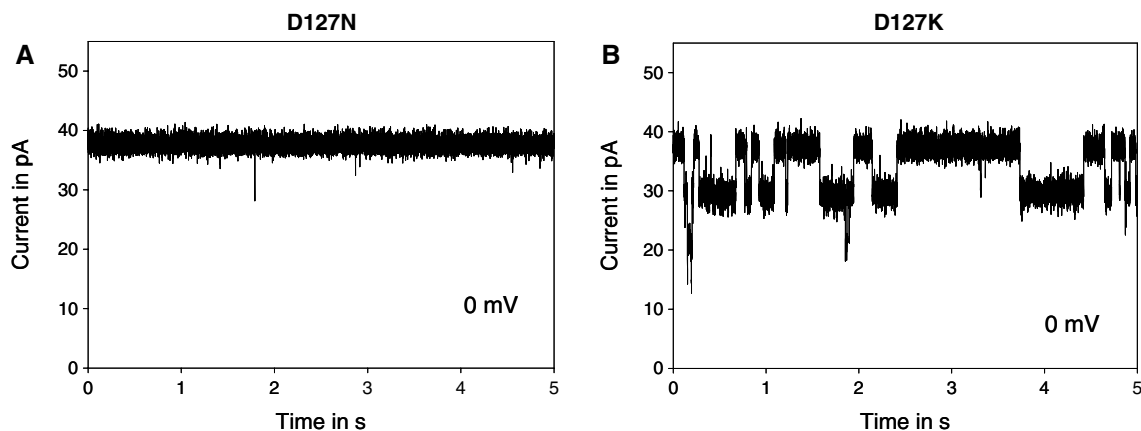


Fig. 4 Current traces of D127N (a) and D127K (b) with no electrical potential applied but with a gradient of 1/0.1 M KCl, pH 7.4 as driving force, equivalent to ~ 52 mV (corrected for ion activi-

ties). Note that the diffusion potential of the 1/0.1 M KCl gradient of ~ 1 mV is neglectable

These observations make us to conclude that residue D127 does not play a dominant role in OmpF voltage gating. To emphasize this conclusion, the current transitions described here are typified consistently as current fluctuations rather than gating events.

Subpopulations with distinct conductance

In contrast to WT conductance, conductance measurements on the two D127 mutants clearly identified the existence of subpopulations. Table 1 lists calculated trimeric slope conductances (at 0 mV and in symmetrical

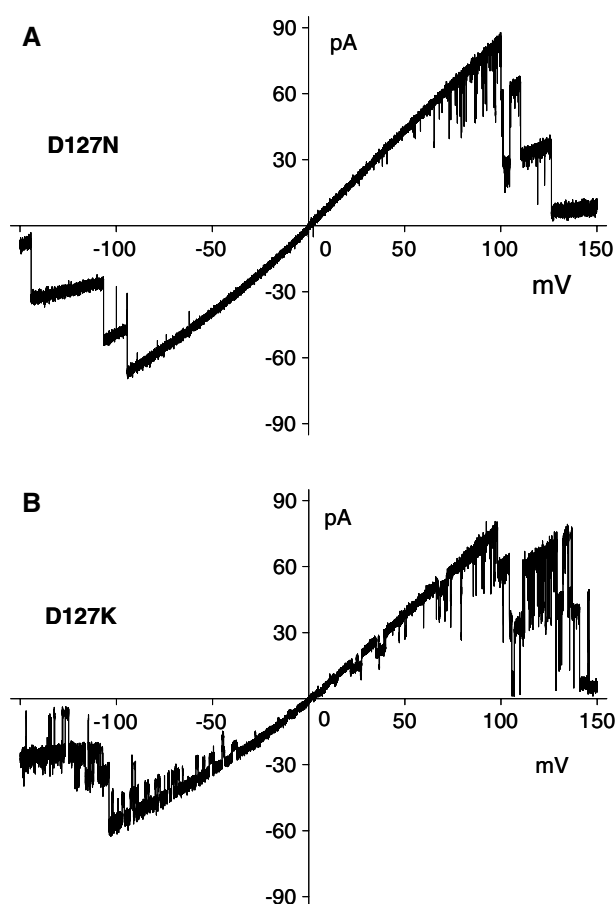


Fig. 5 Current traces of the D127N (a) and D127K (b) mutant in 0.1 M KCl, pH 7.4, in response to a voltage ramp (10 mV/s) from 0 to -150 mV, back to 0 mV (not shown), followed by a ramp from 0 to 150 mV

0.1 M KCl, pH 7.4) after applying the voltage ramp protocol from Fig. 5. As was observed at constant potential (Fig. 2b, c), when exposed to the voltage ramp protocol OmpF mutant, notably D127K, expressed different conductance levels. The data of Table 1 refer to the dominant, i.e., most frequently observed trimeric conductance level of an individual porin protein. Although the subdivision into three (D127N) and two (D127K) subpopulations is somewhat arbitrary, both the relatively large differences between the average values and the relatively small variations in these averages seem to justify the classification. Note that the values in Table 1 slightly differ from the values given in Fig. 2. Bearing in mind the different definition of conductance between the two protocols (current magnitude at -50 and 50 mV versus the slope conductance at 0 mV) and the rectification of OmpF, results are nevertheless considered to be in good agreement. The main difference is the third conductance level found in the D127N mutant when applying the voltage ramp protocol.

Table 1 Calculated slope conductance (g) in symmetrical 0.1 M KCl, pH 7.4 solutions, derived from traces as shown in Fig. 5b, c

	g (pS) 0.1 M KCl
WT	710 ± 6 (14)
D127N	
1	675 ± 9 (8)
2	717 ± 10 (8)
3	787 ± 26 (5)
D127K	
1	593 ± 16 (6)
2	690 ± 10 (5)

Numbers in bold represent subpopulations of each mutant

Selectivity

We also addressed the ion selectivity of the D127 mutants. Results derived from reversal potential measurements (E_{rev}) in 1//0.1 M NaCl, pH 7.4 are summarized in Table 2. As is seen with conductance, both D127N and D127K but not WT show subpopulations with clearly distinct E_{rev} values. The first subpopulation is characterized by an E_{rev} of ~ -11 mV, very similar to that of WT OmpF, and is typified here as ‘low’ selective ($P_{\text{Na}}/P_{\text{Cl}} = 1.8$). E_{rev} of the second subpopulation is, on average, 8 mV more negative (~ -19 mV), and represented here as ‘high’ selective ($P_{\text{Na}}/P_{\text{Cl}} = 2.8$). As already remarked for the conductance data in Table 1, dividing the E_{rev} data into two subpopulations seems justified by the relatively small variations seen in the average values. Although these same two levels of selectivity are found in the two mutants, the distribution of each differs markedly. In D127N, the ‘high’ selectivity prevailed and only 5 out of 22 trimers are found in the ‘low’ selectivity conformation. The ‘low’ selectivity conformation, on the other hand, is dominant in the

Table 2 Measured reversal potentials (E_{rev}) in 1//0.1 M NaCl and 0.01//0.1 M NaCl, pH 7.4

	E_{rev} (mV) 1//0.1 M NaCl	E_{rev} (mV) 0.01//0.1 M NaCl
WT	-12.3 ± 1.1 (15)	45.6 ± 1.5 (6)
D127N		
1	-11.1 ± 0.4 (5)	45.3 ± 1.6 (4)
2	-18.9 ± 2.9 (17)	
D127K		
1	-10.8 ± 2.3 (19)	43.5 ± 1.6 (4)
2	-18.8 ± 1.0 (3)	
D127C	-19.1 ± 2.5 (16)	45.9 ± 1.2 (5)
D127C + MTSEA	-18.7 ± 2.5 (10)	
D127C + MTSET	-18.1 ± 1.7 (8)	

Values were obtained after applying the voltage ramp protocol as used in Fig. 5. Numbers in bold represent subpopulations of each mutant

D127K mutant and here just 3 out of 22 porins express ‘high’ selectivity. Fig. 6 shows reversible switches of selectivity (and conductance) as observed in a single D127K mutant during an E_{rev} measurement. These shifts of E_{rev} are interpreted in terms of a trimeric selectivity that depends on the number of open monomers in a particular conformation (and with a particular selectivity). Note that this is essentially different from an OmpF trimer composed of three monomers with identical selectivity where E_{rev} is independent of the number of open monomers.

All these differences in E_{rev} between WT/D127K and D127N disappeared when similar recordings were performed in a 0.01/0.1 M NaCl gradient (Table 2). Under these lower ionic strength conditions E_{rev} of WT, D127N, D127C and D127K mutant is essentially the same (~ 45 mV) and more cation selective ($P_{\text{Na}}/P_{\text{Cl}} = 20$) compared to the $P_{\text{Na}}/P_{\text{Cl}}$ of 2–3 measured in 0.1 M NaCl.

Accessibility of C127

We were also interested in the accessibility of residue D127. After the substitution of D127 by a cysteine (in the cysteine-free WT OmpF), this D127C mutant was exposed to MTSEA or the slightly larger MTSET, both positively charged (+ 1). Judged from the values of E_{rev} , essentially identical to that of unmodified D127C (Table 2), we conclude that these attempts to chemically modify the D127C pore were all unsuccessful.

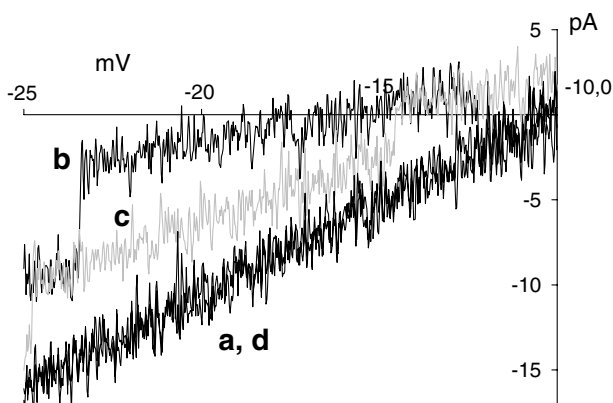


Fig. 6 Reversible transitions of selectivity of the D127K mutant, as visible by shifts of E_{rev} . Trace *a* (black) was recorded first, then traces *b* (black) and *c* (gray) and finally, after E_{rev} had shifted back to its initial value, trace *d* (black, overlap with trace *a*). The observation that E_{rev} depends on which monomers contribute to the total current indicates that all three monomers differ in their selectivity. Traces were recorded in 1/0.1 M NaCl, pH 7.4, using the same voltage ramp protocol as in Fig. 5

Discussion

The present study discusses the protonation state of residue D127 in the context of the functionality of OmpF. As already concluded from its crystal structure (Karsikoff et al. 1994), the side-chain carboxylate is in H-bonding distance (0.26 nm) of the main-chain carbonyl of residue 237, which necessarily implies the protonation of D127. However, outside the crystal and at room temperature the situation may be more dynamic, dependent on the dielectric environment of D127. In fact, a recent detailed MD simulation found that both, a protonated or a charged D127, is energetically feasible (Varma et al. 2006). Regarding to the extent D127 is buried, the inability to chemically modify the D127C mutant with the highly reactive cysteine-dependent MTSEA and MTSET may indicate low accessibility because this residue (and by implication D127 as well) is indeed partly buried. Although this study does not reveal the charge state of D127 in WT OmpF, we are inclined to interpret the results slightly in favor of a deprotonated D127. The D127N mutant is the only protein containing a 127 residue with a rather well-defined charge. Given the occurrence of subpopulations in D127N, one may argue that WT OmpF containing a protonated, also zero-charged D127 would expect to show similar behavior, i.e., showing different conductance and selectivity levels. This is however not what we observed. Actually, of the three proteins studied, WT is the only one that lacks conductance and selectivity subpopulations.

Interestingly, the voltage-independent current fluctuations of D127K described here show strong resemblance with those of previously characterized OmpC mutants. Compared to our D127 OmpF mutants, the D315A OmpC mutant carries a mutation at the other end of the loop, where D315 (i.e., D312 in OmpF) at the barrel wall interacts via hydrogen-bonding with residues E109 and F110 at the tip of L3 (Liu and Delcour 1998). Remarkably, the neutralization of E109 (i.e., E117 in OmpF) instead resulted in much faster fluctuations than those observed in the D315A mutant (Liu et al. 2000). A third OmpC mutant, D118Q (i.e., D126 in OmpF), also showed a variable conductance level, though the fluctuations occurred at much lower frequency than those observed with the D315 and E109 mutants (Liu and Delcour 1998).

The MD studies of Varma et al. (2006) reproduced a cross-sectional area of the eyelet that was identical to the one determined from the crystal structure of OmpF and independent of the charge state of D127. Apart from the subpopulations we observed, that conclusion and our findings can be reconciled in the sense that we identified a (more or less) common conductance level

for WT (710 pS), D127N (717 pS) and the D127K mutant (690 pS).

Although we clearly identified subpopulations of distinct conductance, we only observed a limited number of conductance levels. Given the trimeric nature of OmpF, a two state model for each individual monomer (with distinct conductance) gives four possible combinations (trimers) with different output (conductance). Considering the rather small variation in the conductance data (Table 1), the measurements should have allowed the identification of other levels. How to explain this limited number of subpopulations that was actually identified? One reason seems to be related to statistics. Suppose an OmpF monomer can adopt two conformations with either a 'low' (L) or 'high' (H) conductance. Further, suppose that the current fluctuations in the traces of Fig. 2c reflect transitions between the L and H state of a single monomer. Let P be the probability that a particular monomer occupies the L state. Chances for a trimer to be in the HHH or 'HLH' (i.e., HLH, LHH or HHL) state are $(1 - P)^3$ and $3P(1 - P)^2$, respectively. The probability ratio's, as given by the ratio of surface areas of the all-points histograms (indicated at the base line in Fig. 2d, e), translate in a 26% (at -50 mV) and 21% (at 50 mV) chance for an individual monomer to be in the L state. The probability to catch two ($= 3P^2(1 - P)$) monomers in the L state simultaneously then is 15% (at -50 mV) and 10% (at 50 mV). Chances to find all three monomers in the L state ($= P^3$) at -50 and 50 mV are just < 2 and $< 1\%$, respectively. Based on these numbers we would probably have expected to see more D127K trimers with two monomers in the L state. Actually, only one out of eight D127K trimers analyzed clearly showed all four conductance levels (Fig. 7).

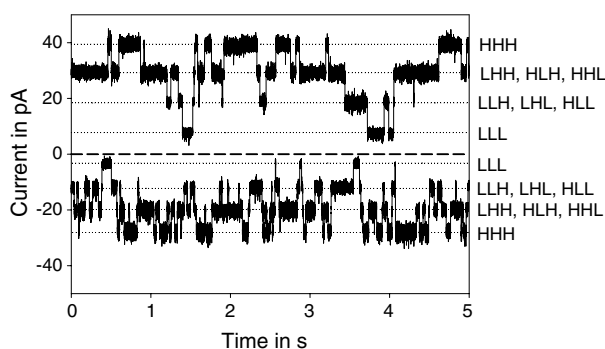


Fig. 7 A D127K trimer (in 0.1 M KCl, pH 7.4 and at ± 50 mV) that shows all four possible conductance levels: all three monomers in the high conductance or H state (HHH), two in H, one in the low conductance or L state (LHH, HLH or HHL), one in H, two in L (LLH, LHL or HLL) or all three in L (LLL). Compare with Fig. 2c in which only two of the four levels are visible (HHH and HLH)

For now, we can only speculate about the origin of current and selectivity fluctuations observed. We will shortly discuss two possible scenarios. As is the case with D127, the pK of a lysine at position 127 may deviate significantly from its value of 10.4 in free solution. As a result, the ionization state of K127 at physiological pH may be rather dynamic. Recently, the proton binding and unbinding of lysine residues in individual nicotinic acetylcholine receptor molecules have been probed electrophysiologically (Cymes et al. 2005). In a similar way, reversible (de)protonations of K127 may cause the current and selectivity level of OmpF (somehow) to fluctuate. Although pH-dependent reversible residue ionization has been studied previously in OmpF, in that study the current fluctuations (recorded as open channel current noise) reached a minimum at neutral pH (Nestorovich et al. 2003). The second scenario we envisage is based on the electrostatic interaction between the residue at position 127 and the nearby R167. Even though D127 (at L3) and R167 (at L4) are too far apart (0.55 nm) to form a salt bridge, electrostatic interaction between these two residues may help to stabilize the position of loop L3. The neutralization of D127 or substitution by a lysine may translate into more (D127N) or less (D127K) stable subconformation states. Apart from the diversity of conductance levels, the lack of flickering of the D127N mutant then suggests that the distinct subconformations observed here are relatively stable: once folded, the D127N protein seems to freeze in that particular conformation. This explains that transition events between these different conformations as in Fig. 2b within a single D127N protein were quite exceptional. In contrast, a positively charged lysine at position 127 introduces significant instability, probably caused by repulsive electrostatics between K127 and R167.

Numerous studies have demonstrated a relationship between the charge constellation in the eyelet and the measured ion selectivity of OmpF (Miedema et al. 2004; Phale et al. 2001; Saxena et al. 1999). Given the location of D127, at the extracellular side of the pore and far remote from the constriction zone, a direct effect of D127 mutations on E_{rev} would not be anticipated. The selectivity differences seen between WT and the D127N/D127K mutants show however that the identity (charge) of residue 127 does have a clear effect on the selectivity of the OmpF channel. One of the main challenges arising from this study is to correlate the two data sets for selectivity and conductance statistically. In the D127N mutant, a high conductance and the high selectivity state prevailed. In contrast, the D127K mutant was found predominantly in a low conductance and the low selectivity state. These

observations are in accordance with a positively charged K127 that lowers both the permeation rate and selectivity of the cation selective OmpF (see also Cymes et al. 2005). However, it does not explain that the D127N mutant is more selective than both WT and the D127K mutant. It neither explains that the D127K mutant shows the same low selectivity as WT OmpF. Apparently, such a consideration based on 'simple' electrostatics is not adequate, suggesting that the effects on selectivity described here are different in nature. There is another indication that points into that direction. Differences between the selectivity of WT/D127K and D127N disappeared after lowering the ionic strength of the solutions. Apparently, under these conditions amino acid residues other than D127 (i.e., residues located in the constriction zone and along the ion permeation pathway) dominate the permeation properties of OmpF. For now, the reason behind the observed distributions of conductance and selectivity remains obscure. Part of the answer may relate to the different ionic conditions the proteins were exposed to during the assessment of selectivity (1/0.1 M NaCl) and conductance (0.1 M KCl). As shown by Alcaraz et al. (2004), the salt species, ionic strength as well as the direction of the salt gradient can affect the ion selectivity and current rectification of OmpF.

In conclusion, the present study shows that the conductance and selectivity of OmpF is rather sensitive to the charged state of the residue at position 127. The differences between D127N and WT seem to be in support of a deprotonated D127 in WT OmpF. According to this view, a charged D127 at the root of loop L3 may contribute to the stabilization of L3. This conclusion may hint that D127, and by implication L3, plays a role in the typical voltage gating of OmpF. A gross movement of L3 as part of the gating mechanism has, however, already been ruled out (Phale et al. 1997). Our results fit in that view: the gating of both D127 mutants show WT-like voltage sensitivity and the current fluctuations of the D127K mutant are voltage-independent. We therefore set these current fluctuations clearly apart from gating events and dismiss residue D127 as a key player in the voltage-sensitive gating mechanism of OmpF.

Acknowledgment This research is supported by NanoNed, a nanotechnology program of the Dutch Ministry of Economic Affairs.

References

- Alcaraz A, Nestorovich EM, Aguilera-Arzo M, Aguilera VM, Bezrukov SM (2004) Salting out the ionic selectivity of a wide channel: the asymmetry of OmpF. *Biophys J* 87:943–957
- Bainbridge G, Gocke L, Lakey JH (1998) Voltage gating is a fundamental feature of porin and toxin β -barrel membrane channels. *FEBS Lett* 431:305–308
- Baslé A, Qutub R, Mehrazin M, Wibbenmeyer J, Delcour AH (2004) Deletions of single extracellular loops affect pH sensitivity, but not voltage dependence, of the *Escherichia coli* porin OmpF. *Protein Eng* 17:665–672
- Bredin J, Saint N, Malléa M, Dé E, Molle G, Pagès J-M, Simonet V (2002) Alteration of pore properties of *Escherichia coli* OmpF induced by mutation of key residues in anti-loop 3 region. *Biochem J* 363:521–528
- Cowan SW, Schirmer T, Rummel G, Steiert M, Ghosh R, Pauptit RA, Jansonius JN, Rosenbusch JP (1992) Crystal structures explain functional properties of two *E. Coli* porins. *Nature* 358:727–733
- Cymes GD, Ni Y, Grosman C (2005) Probing ion channel pores one proton at a time. *Nature* 438:975–980
- Danelon C, Suenaga A, Winterhalter M, Yamato L (2003) Molecular origin of the cation selectivity in OmpF porin: single channel conductances vs. free energy calculation. *Biophys Chem* 104:591–603
- Delcour AH (2003) Solute uptake through general porins. *Front Biosci* 8:1055–1071
- Eisenberg RS (1996a) Computing the field in proteins and channels. *J Membr Biol* 150:1–25
- Eisenberg RS (1996b) Atomic biology, electrostatics and ionic channels. In: Elber R (eds) *New developments and theoretical studies of proteins*, World Scientific, Philadelphia, pp 269–357
- Im W, Roux B (2002a) Ions and counterions in a biological channel a molecular dynamics simulation of OmpF porin: from *Escherichia coli* in an explicit membrane with 1 M KCl aqueous salt solution. *J Mol Biol* 319:1177–1197
- Im W, Roux B (2002b) Ion permeation and selectivity of OmpF porin: a theoretical study based on molecular dynamics, Brownian dynamics, and continuum electrodiffusion theory. *J Mol Biol* 322:851–869
- Karshikoff A, Spassov V, Cowan SW, Ladenstein R, Schirmer T (1994) Electrostatic properties of two porin channels from *Escherichia coli*. *J Mol Biol* 240:372–384
- Klebba PE, Newton SMC (1998) Mechanisms of solute transport through outer membrane porins: burning down the house. *Curr Opin Microbiol* 1:238–248
- Liu N, Delcour AH (1998) The spontaneous gating activity of OmpC porin is affected by mutations of a putative hydrogen bond network or of a salt bridge between the L3 loop and the barrel. *Protein Eng* 11:797–802
- Liu N, Samartzidou H, Lee KW, Briggs JM, Delcour AH (2000) Effects of pore mutations and permeant ion concentration on the spontaneous gating activity of OmpC porin. *Protein Eng* 13:491–500
- Miedema H, Meter-Arkema A, Wierenga J, Tang J, Eisenberg B, Nonner W, Hektor H, Gillespie D, Meijberg W (2004) Permeation properties of an engineered bacterial OmpF porin containing the EEEE-locus of Ca^{2+} channels. *Biophys J* 87:3137–3147
- Nestorovich EM, Rostovtseva TK, Bezrukov SM (2003) Residue ionization and ion transport through OmpF channels. *Biophys J* 85:3718–3729
- Phale PS, Schirmer T, Prilipov A, Lou K-L, Hardmeyer A, Rosenbusch JP (1997) Voltage gating of *Escherichia coli* porin channels: role of the constriction zone. *Proc Natl Acad Sci USA* 94:6741–6745
- Phale PS, Philippssen A, Widmer C, Pahe VP, Rosenbusch JP, Schirmer T (2001) Role of charged residues at the OmpF

- porin channel constriction probed by mutagenesis and simulation. *Biochemistry* 40:6319–6325
- Philippsen A, Im W, Engel A, Schirmer T, Roux B, Müller DJ (2002) Imaging the electrostatic potential of transmembrane channels: atomic probe microscopy of OmpF porin. *Biophys J* 82:1667–1676
- Robertson KM, Tieleman DP (2002) Molecular basis of voltage gating of OmpF porin. *Biochem Cell Biol* 80:517–523
- Saint N, Lou K-L, Widmer C, Luckey M, Schirmer T, Rosenbusch JP (1996) Structural and functional characterization of OmpF porin mutants selected for larger pore size. *J Biol Chem* 271:20676–20680
- Saxena K, Drosou V, Maier E, Benz R, Ludwig B (1999) Ion selectivity reversal and induction of voltage-gating by site-directed mutations in the *Paracoccus denitrificans* porin. *Biochemistry* 38:2206–2212
- Schindler H, Rosenbusch JP (1978) Matrix protein from *Escherichia coli* outer membranes forms voltage-controlled channels in lipid bilayers. *Proc Natl Acad Sci USA* 75:3751–3755
- Schirmer T (1998) General and specific porins from bacterial outer membranes. *J Struct Biol* 121:101–109
- Schirmer T, Phale PS (1999) Brownian dynamics simulation of ion flow through porin channels. *J Mol Biol* 294:1159–1167
- Schulz GE (2002) The structure of bacterial outer membrane proteins. *Biochem Biophys Acta* 1565:308–317
- Tieleman DP, Berendsen HJC (1998) A molecular dynamics study of the pores formed by *Escherichia coli* OmpF porin in a fully hydrated plamitoyloleoylphosphatidylcholine bilayer. *Biophys J* 74:2786–2801
- Todt JC, McGroarty EJ (1992) Involvement of Histidine–21 in the pH-induced switch in porin channel size. *Biochemistry* 31:10479–10482
- Todt JC, Roqueand WJ, McGroarty EJ (1992) Effects of pH on bacterial porin function. *Biochemistry* 31:10471–10478
- Van Gelder PN, Saint N, Phale PS, Eppens EF, Prilipov A, van Boxel R, Rosenbusch JP (1997) Voltage sensing in the PhoE and OmpF outer membrane porins of *Escherichia coli*: role of charged residues. *J Mol Biol* 269:468–472
- Varma S, Jakobsson E (2004) Ionization states of residues in OmpF and mutants: effects of dielectric constant and interactions between residues and ionic strength. *Biophys J* 86:690–704
- Varma S, Chiu S-W, Jakobsson E (2006) The influence of amino acid protonation states on molecular dynamics simulations of the bacterial porin OmpF. *Biophys J* 90:112–123
- Vrouenraets M, Wierenga J, Meijberg W, Miedema H (2006) Chemical modification of the bacterial porin OmpF: gain of selectivity by volume reduction. *Biophys J* 90:1202–1211